ISBN: 978-3-95450-184-7 doi:10.18429/JACoW-IPAC2018-THPMK108

PRODUCTION OF MAGNETIZED ELECTRON BEAM FROM A DC HIGH VOLTAGE PHOTOGUN*

M. A. Mamun†, P. Adderley, J. Benesch, B. Bullard, J. Delayen[1], J. Grames, J. Guo, F. Hannon, J. Hansknecht, C. Hernandez-Garcia, R. Kazimi, G. Krafft[1], M. Poelker, R. Suleiman, M. Tiefenback, Y. Wang[1], S. Zhang, Thomas Jefferson National Accelerator Facility, Newport News, VA-23606, USA
S. Wijethunga, Old Dominion University, Norfolk, VA 23529, USA
[1]also at Old Dominion University, Norfolk, VA 23529, USA

Abstract

Bunched-beam electron cooling is a key feature of all proposed designs of the future electron-ion collider, and a requirement for achieving the highest promised collision luminosity. At the Jefferson Lab Electron Ion Collider (JLEIC), fast cooling of ion beams will be accomplished via so-called 'magnetized cooling' implemented using a recirculator ring that employs an energy recovery linac. In this contribution, we describe the production of magnetized electron beam using a compact 300 kV DC high voltage photogun with an inverted insulator geometry, and using alkali-antimonide photocathodes. Beam magnetization was assessed using a modest diagnostic beamline that includes YAG view screens used to measure the rotation of the electron beamlet passing through a narrow upstream aperture. Magnetization results are presented for different gun bias voltages and for different laser spot sizes at the photocathode, using 532 nm lasers with DC and RF time structure. Photocathode lifetime was measured at currents up to 4.5 mA, with and without beam magnetization.

INTRODUCTION

The process "electron cooling" is an important feature of proposed designs of the nation's future Electron Ion Collider (EIC) [1]. Electron cooling is used to transfer unwanted transverse motion of individual ions within ion bunches to a sacrificial "cold" electron beam. When implemented, ion bunches occupy a smaller volume in space and time, resulting in improved luminosity when the ion bunches eventually collide with the electron bunches of a physics beam. Electron cooling has been implemented at a number of laboratories, such as Fermi Lab [2], but not under the extremely demanding conditions required by the EIC [1]. An innovative cooling method promises to meet EIC cooling requirements by delivering an electron beam to a long solenoid magnet through which the ion beam passes [3, 4]. Inside the solenoidal field, the electrons would follow small helical trajectories thereby increasing the interaction time with ions and improving the cooling efficiency by up to two orders of magnitude over previously demonstrated cooling techniques. But delivering the electron beam into the cooling solenoid represents a significant challenge. The fringe field immediately upstream of the cooling solenoid "kicks" the electron beam, introducing a large deviation from the desired trajectory of the electron beam inside the solenoid. It is expected that the ill-effects of this fringe field can be cancelled if the electron beam is born in a similar field, and passing through a fringe field at the exit of the photogun that produces a beam motion "kick" in the opposite direction, such that the two "kicks" cancel.

In this work an electron beam was generated from a DC high voltage photogun where the bialkali antimonide photocathode that was immersed in a solenoidal field – so-called 'magnetized beam' – and characterized for beam magnetization as a function of solenoid field involving beam size and beam rotation measurements using a slit and viewer method for different laser spot sizes and locations. The experimental results are compared to prediction. Lifetime of magnetized and non-magnetized beam was also assessed.

EXPERIMENTAL SETUP

The magnetized electron source consists of bialkali antimonide photocathode, gun HV chamber, gun solenoid, 532 nm RF-pulsed laser, and beamline with diagnostics (Fig. 1).

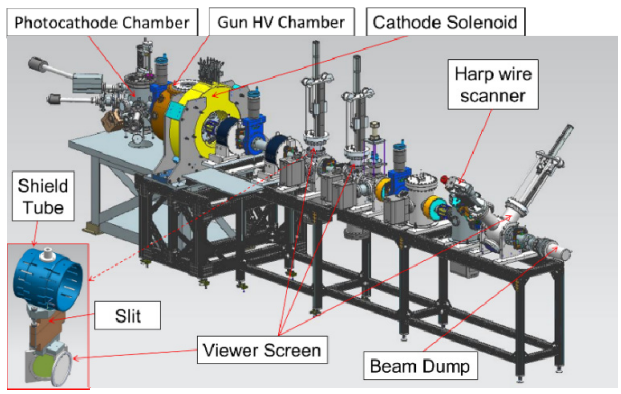

Figure 1: Beamline setup, slit and view screen (inset).

Photocathode Deposition Chamber

A load-lock type bialkali antimonide photocathode deposition chamber was built and installed behind the gun high voltage chamber. The technical details of key com-

* Authored by Jefferson Science Associates, LLC under U.S. DOE Contract No. DE-AC05-06OR23177. Additional support comes from Laboratory Directed Research and Development program. The U.S. Government retains a non-exclusive, paid-up, irrevocable, world-wide license to publish or reproduce this manuscript for U.S. Government purposes.
† mamun@jlab.org

ISBN: 978-3-95450-184-7 doi:10.18429/JACoW-IPAC2018-THPMK108

ponents of the deposition system and process are similar to [5]. Chamber vacuum of ~ 9×10^{-10} Pa was achieved and maintained with the help of non-evaporable getter (NEG) pumps, ion pumps backed up by turbomolecular pump and following ~ 100 h vacuum bake at 190 °C. The deposition chamber was equipped with an RGA mass spectrometer (SRS model RGA200) to continuously monitor the vacuum gas composition and it also served as a deposition monitor for the photocathode chemical species. Pure elemental sources of Sb, Cs, and K were thermally evaporated and deposited onto p-doped <110> GaAs substrates mounted on molybdenum "pucks". The deposition chamber was equipped with two resistive heaters attached to long stalks and mounted on linear translation stages: one at the bottom and one at the top of the chamber. The bottom heater was used for heat cleaning the substrate at ~ 450 °C for at least 18 h, while the top heater was used to maintain the surface deposition temperature at ~ 120 °C. Pucks face up during substrate cleaning, and face down during photocathode preparation. The top heater was mounted on a short ceramic nipple that enabled maintaining a negative bias (−280 V) during deposition process to monitor photoemission evolution. During deposition, the substrate was lowered from the parking position to a working distance of 3 cm from the sources.

The photocathode was activated in a two-step process where a thin Sb film deposition is followed by simultaneous deposition of alkalis from an effusion source. The Sb source was resistively heated by supplying 25 A current through a tungsten wire wrapped around an alumina crucible containing Sb pellets. The Sb deposition time was varied from 10 to 20 min to vary the Sb film thickness. Photocurrent was continuously monitored using a low power (4 mW) 532 nm green laser during alkali deposition. The alkali deposition was discontinued when the photoemission current reached a maximum. Typical quantum efficiency (QE) values were in the range of 5 to 8% at 532 nm. A mask with 3 and 5 mm aperture sizes was used to limit the photocathode active area within the full area (13 mm dia.) of the substrate. Limited active area is desired to reduce beam halo, minimize vacuum excursions and high voltage arcing, and prolong photogun operating lifetime. Once a photocathode was prepared, it was quickly transferred to the photogun cathode electrode via a magnetic sample manipulator.

DC High Voltage Photogun

A load-lock type compact DC high voltage photogun with inverted insulator and spherical cathode electrode with a screening shed was designed, built and installed for this study. The compact design helped to reduce the outgassing load and the screening shed electrode helped lower the electric field strength at the triple point junction from 100 MV/m to less than 10 MV/m at 350 kV. The screening electrode also helped to linearize the potential along the tapered insulator which was 17.8 cm long and made of 94% purity doped alumina. The spherical cathode and screening electrodes were centrifugal barrel polished in just one hour to achieve a mirror-like surface finish compared traditional sand paper and diamond paste polishing that requires 30 days. The cathode/anode gap was 9 cm. The gun components were SRF cleaned, assembled and baked at 190 °C for ~ 100 h. The gun was equipped with NEG pumps and ion pump and the post-bake vacuum was maintained at ~ 2×10^{-11} Pa. A 500 kV DC Cockcroft-Walton SF_6 gas–insulated high voltage power supply with a 300 MΩ conditioning resistor in series was employed to energize the photogun. The gun was high voltage conditioned and Kr gas processed to eliminate field emitters. The photogun was conditioned to 360 kV and operated at or below 300 kV. Further details on the photogun are reported in [6].

Cathode Solenoid Magnet

To magnetize the electrons, a solenoid magnet was positioned at the front of the gun chamber, 0.2 m away from the photocathode. The solenoid does not have a steel shield. The solenoid dimensions are 11.8″ ID, 27.6″ OD, and 6.2″ width (z), comprised of 16 layers of 20 turn water-cooled copper conductor with a cross section area of 0.53 cm^2 and total length of 500 m. The conductor has 0.18 Ω resistance (65 °C average T). The solenoid was energized with a spare CEBAF Dogleg magnet power supply (400 A, 79 V) and can provide magnetic field to 1.5 kG at the photocathode. A magnetic model using Opera was developed that includes the gun solenoid and other magnetic components along the beamline. The effect of the steel solenoid casings on the focusing beamline solenoids distorts the field of the magnetizing solenoid [7]. First trials of energizing cathode solenoid with photogun at high voltage resulted in new field emission and vacuum activity. Later a procedure was developed and followed to energize cathode solenoid without exciting new field emitters.

Diagnostic Beamline

The beamline extends ~ 4.6 m from the gun photocathode and includes two fluorescent YAG screens in combination with slits and a third YAG screen located at 1.5, 2.0 and 3.75 m respectively. The YAG screens and slits are used to measure the transverse density profile and to trace the beam rotation angles. The beamline has seven steering magnets and four focusing solenoids to compensate space-charge emittance growth and to transport the beam to the Faraday Cup beam dump for photocathode lifetime measurements at milliampere beam current. A 532 nm green rf-pulsed drive laser was used for all measurements (374 MHz bunch repetition rate, and ~ 35 ps pulsewidth FWHM). The laser beam temporal profile was Gaussian and the laser spot size was varied using focusing lens in the laser transport.

The beam size and beam rotation angle were measured as a function of solenoid field (up to 1.5 kG) by varying solenoid supply current to 400 A. The rotation angle was obtained by passing a beamlet through an inserted slit at either of the first two view screen locations and measuring the orientation of drifted beamlet at a downstream view screen. Magnetized and nonmagnetized beam (at

ISBN: 978-3-95450-184-7 doi:10.18429/JACoW-IPAC2018-THPMK108

300 kV and with all beamline focusing solenoids set off) were investigated for different laser spot sizes (0.1 and 0.3 mm rms) and radial locations (0 and 5 mm from center of cathode). Recorded image data were post-processed using a MATLAB curve fitting tool to determine angular rotation. Lifetime of milliampere beams (up to 4.5 mA) were studied under different gun bias voltages, laser spot sizes, and beam currents.

RESULTS AND DISCUSSION

Figure 2 illustrates representative beam images on two view screens (separated by 0.5 m) and the corresponding drifted beamlet for nonmagnetized and magnetized beam (1.5 kG).

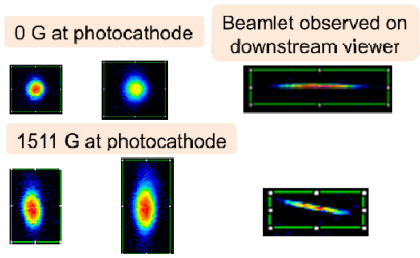

Figure 2: Image of beam and beamlet on viewers.

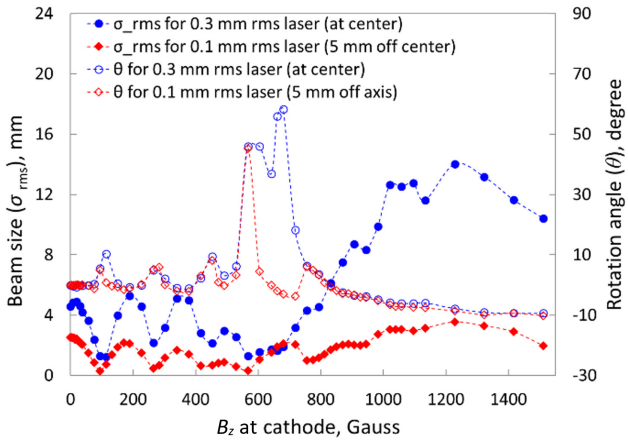

Figure 3: Beam rms size (at view screen 2) and rotation angle (slit 1 to view screen 2) of electron beam measured on as a function of magnetic field on the photocathode.

Figure 3 summarizes the measurements at the second YAG screen for beamlet passing through the first slit, showing beam sizes and corresponding beamlet rotation angles versus magnetizing solenoid field strength. A non-uniform cathode magnetic field causes mismatch oscillations [8], which describes the imbalance between the initial emittance force and applied magnetic force on photocathode, resulting in repeated focusing inside the solenoid field which affects the beam size at the exit of the solenoid field and resulted in varying beam expansion rate in the field free region. Above behaviour is evident from the observed oscillating beam profiles and the corresponding beam rotation. The measured data were further used for modelling the beamline and simulation results are reported in [7, 8].

A charge lifetime of 164.2 C for the magnetized beam (1.5 kG at cathode) was measured at 4.5 mA during a seven hour run, where QE decreased gradually from 7.5−4.5 % [8]. This charge lifetime is less than other reported values using similar photocathode, and could possibly be attributed to the poor thermal conductivity of GaAs substrate. Further measurement of charge lifetime from 22 runs of hour-long duration at currents between 3 and 4.5 mA, using a 0.3 mm rms laser spot under different conditions (200−300 kV gun HV, and 0−400 A cathode solenoid current revealed no correlation between lifetime and gun HV, magnetization, or run sequence. However, better lifetime was observed at lower beam current, good initial QE, and for lower laser power. We experienced sudden QE loss due to arcing and this happened only with non-magnetized beam. Strong focusing effect of cathode solenoid might help keep ions away from the electron beam.

CONCLUSION AND FUTURE PLAN

In summary, magnetized beam was generated from a 300 kV DC photogun and characterized with a modest diagnostic beamline. Beam magnetization was studied as a function of applied magnetic field (up to 1.5 kG) at the photocathode by measuring beam sizes and beam rotation angle using a slit and view screen approach. Non-uniform magnetic field causes the mismatch oscillation. Consequently, focusing of beam was observed in addition to magnetization, and the rotation angle was influenced by Larmor oscillation. Future measurements of beam emittance versus magnetic fields and beam sizes at photocathode will help to evaluate angular momentum. Magnetized beam at 4.5 mA was demonstrated and a limited charge lifetime of 164.2 C was obtained. Further lifetime measurements will be studied soon for the photocathode grown on a molybdenum substrate which is expected to enhance charge lifetime due to better heat dissipation. We plan to run high current beams with bunch charge up to 3 nC using the regenerative amplifier laser and characterize the effect of space charge on beam magnetization. We also plan to implement non-invasive magnetic momentum monitoring using a TE_{011} Cavity.

ACKNOWLEDGMENTS

Authored by Jefferson Science Associates, LLC under U.S. DOE Contract No. DE-AC05-06OR23177 and supported by Laboratory Directed Research and Development funding. The U.S. Government retains a non-exclusive, paid-up, irrevocable, world-wide license to publish or reproduce this manuscript for U.S. Government purposes.

REFERENCES

[1] A. Accardi et al., Electron-Ion Collider: The next QCD frontier, arXiv:1212.1701 (2012).

[2] A. Shemyakin, and L. R. Prost, “The Recycler Electron Cooler,” 2013.

[3] Ya.S. Derbenev, Nucl. Instr. and Meth. A **441,** 223 (2000).

[4] P. Piot et al., Generation and Dynamics of Magnetized Electron Beams for High-energy Electron Cooling, FERMILAB-CONF-14-142-APC.

ISBN: 978-3-95450-184-7 doi:10.18429/JACoW-IPAC2018-THPMK108

[5] M.A. Mamun et al., J. Vac. Sci. Technol. A **34,** 021509 (2016); doi: 10.1116/1.4939563.

[6] Y. Wang, et al., "300 kV DC High Voltage Gun with Inverted Insulator Geometry & CsK_2Sb Photocathode", presented at the 9th Int. Particle Accelerator Conf. (IPAC'18), Vancouver, Canada, Apr.-May 2018, paper SUSPF028, this conference.

[7] S. Wijhetunga, et al., "Simulation Study of the Magnetized Electron Beam", presented at the 9th Int. Particle Accelerator Conf. (IPAC'18), Vancouver, Canada, Apr.-May 2018, paper SUSPF086, this conference.

[8] M. Reiser, Theory and Design of Charged Particle Beams (Wiley, New York, 2008).